Results

PSD-95 shRNA

To address the unsolved question of PSD-95 function I used short hairpin RNA (shRNA) to knock-down protein expression. shRNA mediated knock-down of protein expression is one of the established methods exploiting the naturally occurring expression control mechanism known as RNA interference (RNAi). Cells express shRNAs that are complementary to the mRNA they control. The shRNAs are processed and bound by two complexes called DICER (***) and RISC. Subsequentially the complementary the RISC complex binds the mRNA and the mRNA is degraded. This mRNA depletion decreases the protein level. In shRNA experiments, the short hairpin RNAs are expressed from a DNA plasmid vector. Polymerase III promoters are generally used as they reliably terminate transcription.

shRNA constructs affect the targeted mRNA with variable efficiency. I generated four potential shRNA constructs to suppress PSD-95 expression. To test for efficiency I co-expressed the shRNA together with PSD-95 cDNA in HEK293T cells. I used the shRNA vector without a hairpin insert as a control to visualize unaffected PSD-95 expression.

I determined the PSD-95 expression level by Western blot analysis. Actin serves as loading control. Construct #1, 2 and 4 yield very good to moderate knock-down (Figure 7A). Construct #3 appears to have no effect on PSD-95

expression. PSD-95 shRNA construct #1 is the most efficient and will be referred to as PSD-95 shRNA below.

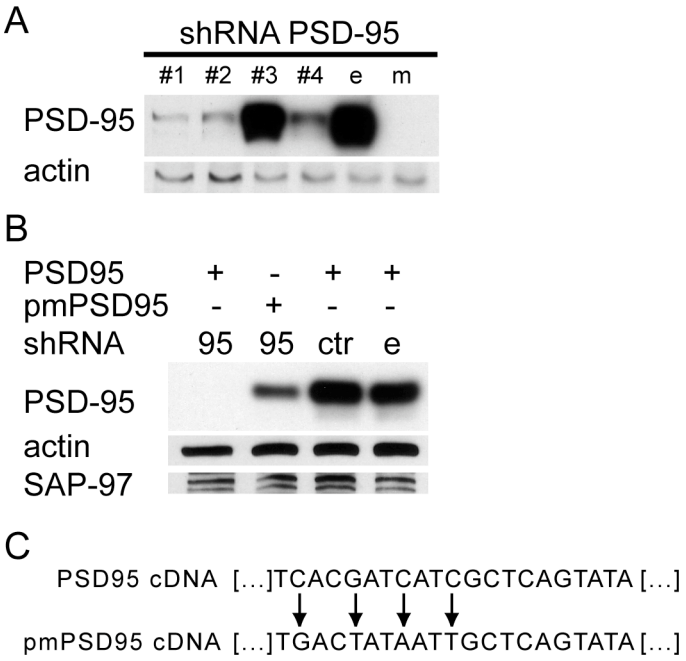

Figure 7 shRNA against PSD95 selectively reduces PSD-95 expression in HEK cells. A) #1, #2 and #4 shRNA sequences reduce PSD-95 expression compared to control levels. Number one is selected for highest efficiency. Vector without shRNA insert is used as control (e). Mock transfection (m) visualizes native expression of PSD-95. B) shRNA PSD-95 reduces expression of native but not PSD-95 cDNA containing silent point mutations. Introduction of silent point mutations into PSD-95 cDNA at the shRNA annealing region abolishes knock-down effect of shRNA. A control shRNA sequence (ctr) has no effect on PSD-95 expression when compared to empty vector control (e). C) Four translationally silent point mutations are introduced into PSD-95 cDNA at the region targeted by the shRNA. Incomplete annealing of the RNAi abolishes efficient degradation of PSD-95 mRNA.

One major concern regarding RNAi is the proof of target specificity. Two control experiments prove target specificity: One, an unrelated control sequence (ctr) does not reduce PSD-95 expression in HEK cells (Figure 7B). Two, to prove that the loss of PSD-95 expression is due to direct interaction of the targeting hairpin with the mRNA, I introduced silent point mutations into the PSD-95 mRNA (pmPSD-95) at the region that anneals to the shRNA to rescue PSD-95

expression. Introduction of mismatches prevents shRNA annealing and subsequent mRNA degradation. pmPSD-95 expression is not effected by the targeting shRNA (Figure 7C). This rescue experiment proves target specificity of the PSD-95 shRNA in HEK293T cells.

PSD-95 knock-down in neurons

Can shRNA knock-down PSD-95 expression in primary hippocampal neurons? Cultured hippocampal neurons are transfected with PSD-95 shRNA vector at 10 to 12 days *in vitro* (DIV 10-12) and incubated for 5 more days. I stained the neurons for PSD-95 and for other postsynaptic markers, PSD-93 and Homer (Figure 8A-B). Transfected cells are compared to untransfected neighboring cells. GFP is expressed in tandem from the shRNA vector and serves as transfection marker. Under control conditions PSD-95 co-localizes almost completely with PSD-93 or Homer at postsynaptic densities. In shRNA transfected neurons PSD-95 is not detected. Postsynaptic markers PSD-93 or Homer are not affected by shRNA PSD-95 expression.

Expression of a control shRNA shows no effect on PSD-95 expression (Figure 8C). Co-localization with PSD-93 is reduced to about 15% in shRNA PSD-95 expressing cells with almost complete overlap in control sequence expressing and non transfected cells (Figure 8D). This data shows specific reduction of PSD-95 below detectable levels. To rescue expression of PSD-95 in neurons after shRNA mediated knock-down, I generated a pmPSD-95-GFP fusion construct expressed from the same vector as the shRNA targeting PSD-95.

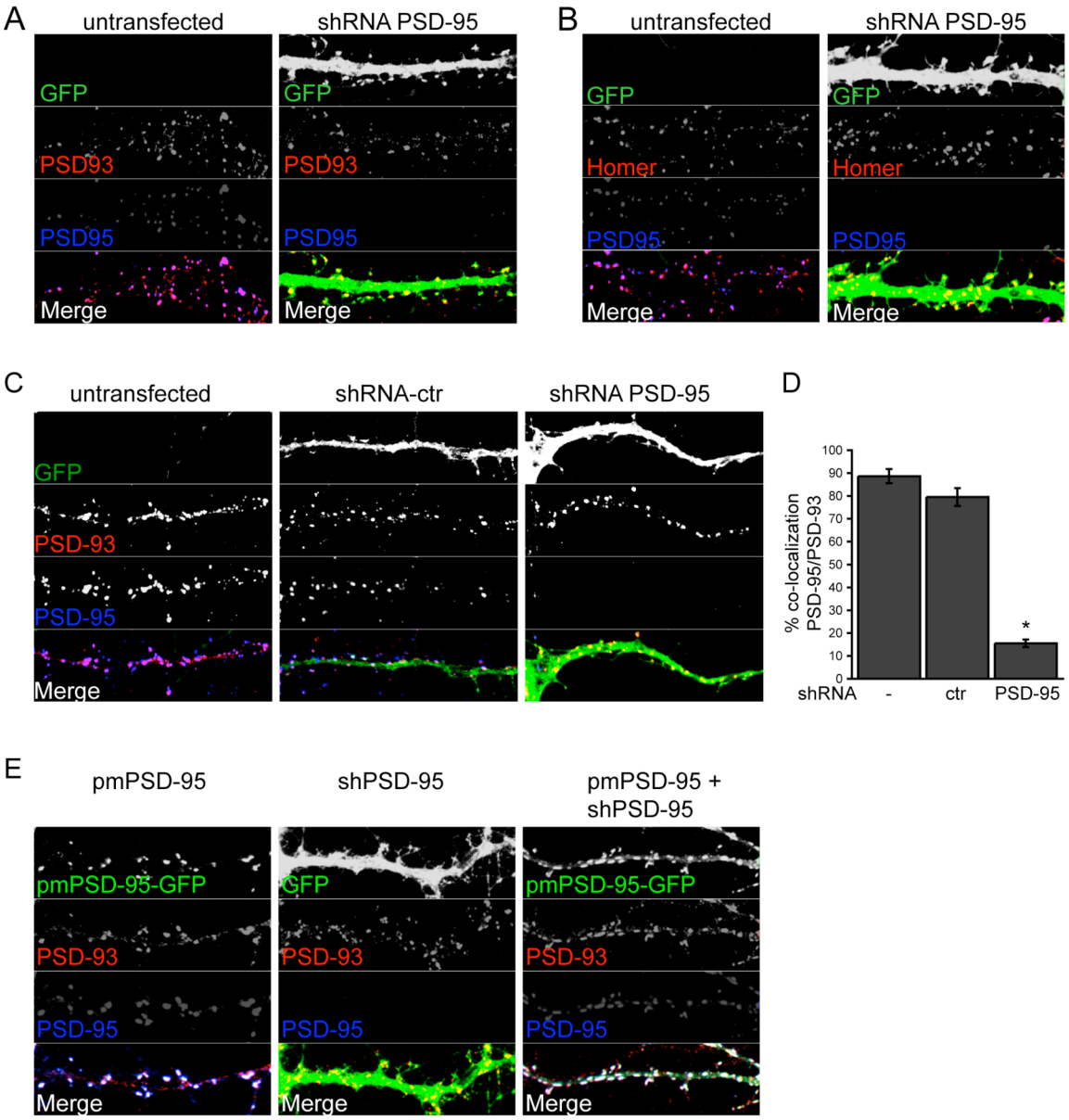

Figure 8 Loss of PSD-95 by shRNA mediated knock-down is efficient and specific. A-B) PSD-95 is absent from neurons transfected with shRNA targeting PSD-95. Other postsynaptic markers PSD-93 and Homer are not affected. C) Co-localization of PSD-95 and PSD-93 is abolished by PSD-95 shRNA but not control shRNA sequence. D) Quantification of PSD-95 and PSD-93 co-localization is lost by shRNA targeting PSD-95. E) Expression of pmPSD-95 rescues knock-down of native PSD-95. PSD-95 and pmPSD-95-GFP co-localize when expressed without shRNA (left). pmPSD-95-GFP expression is not effected by shRNA PSD-95 (right) when compared with control conditions (middle).

This is necessary to ensure each transfected cell carries both the shRNA and pmPSD-95-GFP. GFP is used as a marker for transfection. PSD-95 shRNA

reduces PSD-95 levels significantly but has no effect on pmPSD-95-GFP proving target specificity through direct interaction of shRNA and mRNA in primary neurons (Figure 8E).

Loss of PSD-95 reduces surface glutamate receptor 2 (GluR2)

After establishing effective and specific knock-down of PSD-95 I assessed the effect of loss of PSD-95 on GluR2, a major subunit of AMPARs in the hippocampus. PSD-95 has been proposed to function as the molecular anchor of the AMPAR complex at the excitatory synapses of hippocampal neurons. Thus loss of PSD-95 should lead to a reduction of AMPARs from synapses.

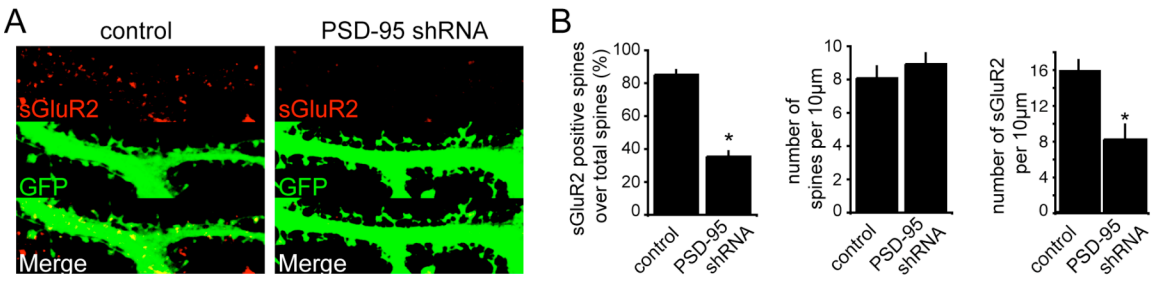

Figure 9 shRNA PSD-95 reduces surface GluR2 expression A) Surface GluR2 stained shRNA PSD-95 and control transfected neurons. Surface GluR2 expression is impaired in shRNA PSD-95 only. GFP co-expressed from the same vector visualizes morphology. B) Quantification of sGluR2 puncta. Number of puncta located on an excitatory spine is reduced to about 40% in shRNA PSD-95 transfected neurons compared to control conditions. There is no change in total spine number (middle). Total sGluR expression is also effected to about 50% of control (right).

I tested this hypothesis with the surface GluR2 staining assay (88). Live cultured hippocampal neurons are incubated for a short period of time with antibodies against the extracellular N-terminal domain of GluR2. The cells are then stained with secondary fluorescently labeled antibodies (Figure 9A). Knock-down of PSD-95 results in the loss of ~50% of surface GluR2 including sGluR2

on spine heads – the location of excitatory synapses (Figure 9B). There is no change in total spine number accompanying this loss of AMPAR (Figure 9B middle panel), but the total number of dendritic surface GluR2 puncta is reduced (Figure 9B right panel). In conclusion shRNA against PSD-95 efficiently suppresses PSD-95 expression and does reduce the number of synaptic GluR2 receptors.

Function of PSD-MAGUK family members

As described in the introduction, the functions of the four PSD-MAGUK family members have been the topic of intense debate. Studies have suggested common as well as distinct roles for each isoform at the excitatory synapse. The experiments above provide the tools to assess each individual isoform in a broader study. I will present some of the data on PSD-95 shRNA again as a positive control.

Identification of efficient shRNAs for all PSD-MAGUKs

For each PSD-MAGUK I generated four potential targeting constructs. Their efficiency was tested by co-expression of the shRNA with the corresponding cDNA. In contrast to the experiments above, COS-7 cells were used for the shRNA SAP97 assay to avoid background effects on SAP97 highly expressed in HEK293T cells[*].

[*] Native SAP97 expression in HEK293T cells is not effected by this shRNA due to sequence differences in this human origin derived cell line.

The initial screen yields at least one efficient shRNA for each of the PSD-MAGUKs. I selected PSD-95 #1, PSD-93 #4, SAP97 #4 and SAP102 #3 and will refer to them as shRNA of the respective proteins below (Figure 10). Actin served as control for equal loading.

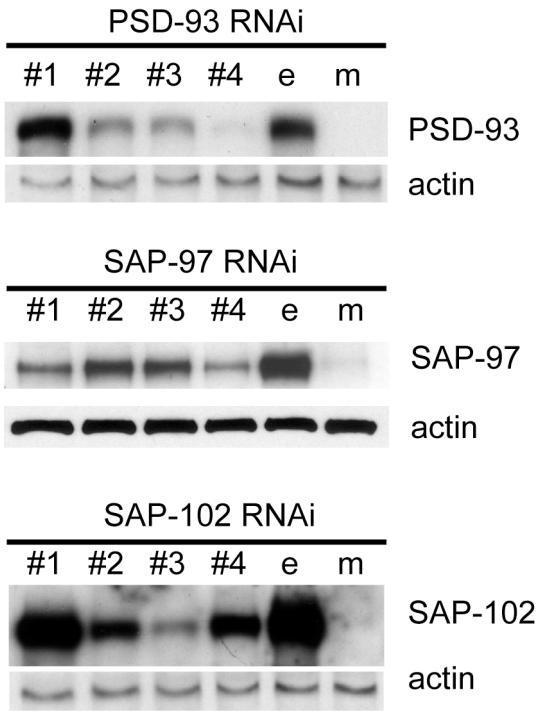

Figure 10 At least one shRNA efficiently knocks down PSD-93, SAP97 and SAP102. cDNAs for PSD-93, SAP97 or SAP102 are co-expressed with the respective shRNA targeting constructs in HEK293T or COS-7 cells (#1-#4). Two days after transfection total cell lysate is assayed by Western blot analysis. PSD-93 #4, SAP97 #4 and SAP102 #3 are selected and referred to as shRNA PSD-93, SAP97 and SAP102 respectively. Western blot for actin shows equal loading.

Each PSD-MAGUK shRNA is target specific

To prove direct interaction of the shRNAs with it targeted mRNA, I generated silent point mutations in each of the targeted cDNAs in the region annealed with the shRNA.

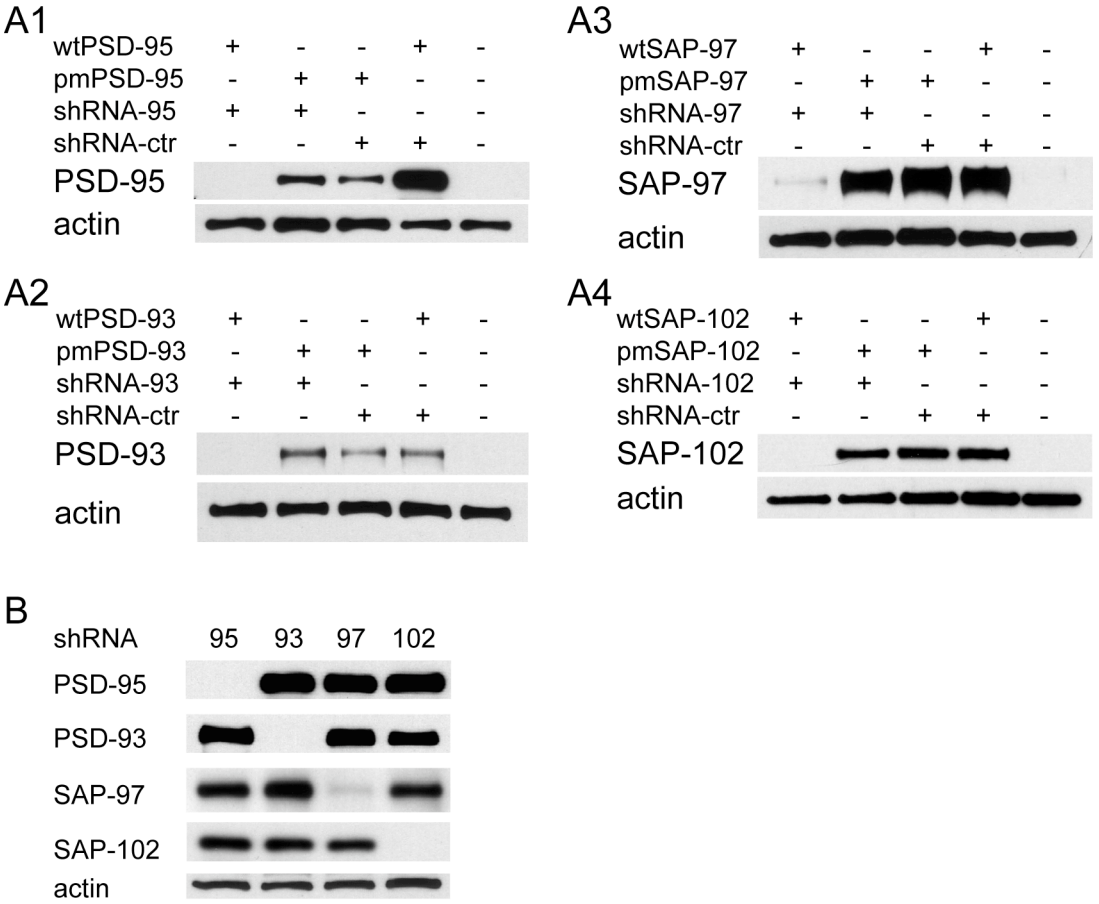

Figure 11 shRNAs against PSD-MAGUKs are target and isoform specific. A) Western blots of PSD-MAGUKs show, point mutant cDNAs rescue expression of shRNA targeted PSD-MAGUKs. Wildtype (wt) or point mutant (pm) PSD-MAGUK cDNAs are co-expressed with targeting or control shRNAs in COS-7 cells. shRNAs suppress expression of wildtype but not point mutant cDNA. Neither wildtype nor point mutant cDNA expression is effected by control shRNA. Lysate of mock transfected COS-7 cells is shown to determine background expression of PSD-MAGUKs. A1) PSD-95 A2) PSD-93 A3) SAP97 and A4) SAP102. Western blots of actin control for equal loading. B) shRNAs do not effect expression of other isoforms as shown by western blots. cDNAs of each PSD-MAGUK are co-expressed with each shRNA targeting PSD-MAGUKs in turn. shRNAs repress expression of targeted isoform only with no effect on other PSD-MAGUK isoforms. An example of actin control western blot is shown to indicate equal loading.

I performed rescue experiments with these constructs. The chosen shRNAs were unable to knock-down point mutant PSD-MAGUK expression. Furthermore, no effect on expression for either point mutant PSD-MAGUK or the native cDNAs was observed when over expressed alongside a control shRNA.

Selected shRNA for PSD-95 (Figure 11A1) PSD-93 (Figure 11A2), SAP97 (Figure 11A3) and SAP102 (Figure 11A4) are efficient and target specific. Actin serves as loading control.

Isoform specificity of shRNA PSD-MAGUKs

PSD-MAGUKs are highly homologous on both protein and DNA levels. To determine the individual functions of the members of the PSD-MAGUKs, it is of important to determine isoform specificity for each shRNA. That is, none of the shRNAs should affect the expression of any of PSD-MAGUKs. I expressed each shRNA identified above with each individual cDNA of the PSD-MAGUKs to test for isoform specificity (Figure 11B). Each shRNA proved isoform specific with no effect on other PSD-MAGUKs.

Knock-down in hippocampal cultures

Selected shRNAs proved efficient and selective in the heterologous cell system. But does this hold true in neurons? I was unable to test all shRNA constructs by transfection, followed by immunohistochemistry due to the fact that the antibodies used to detected SAP97 and SAP102 do not work in this assay reliably (data not shown). I therefore had to establish a Western blot based detection system for knock-down in cultured hippocampal neurons. Neurons are not readily transfected with high efficiency with reagents currently available, but they can be infected with high titer lentivirus derived particles. Lentivirus based

vectors can infect non dividing cells that are difficult to transfect. They integrate stably into the genome allowing longer observations. As they are capable of infecting almost any cell type, they pose a significant safety issue. The newest generation of lentivirus based vectors is replication incompetent, as they lack vital components and are produced from three to four separate vectors to minimize the risk of genome reassembly. One other advantage of viral infection is the freedom to choose the time point of infection during the maturation process of neurons in culture. I therefore established a protocol to generate high titer lentivirus particles.

High titer lentivirus particle

The experiments described below require high titer lentivirus particles for two reasons. One, lentiviruses can infect a target cell multiple times. To high infection rate, many more viral particles than targeted cells are needed. Second, cultured neurons are sensitive to changes in their environment. Ideally the smallest possible volume is added to deliver sufficient amounts of infectious particles. Multiple factors influence the amount of viral particles produced in a culture system. HEK 293T cells have been engineered for optimized protein expression. I based my optimization on this cell line. Other factors are the amount of DNA transfected, the transfection reagent and media used to produce the particles.

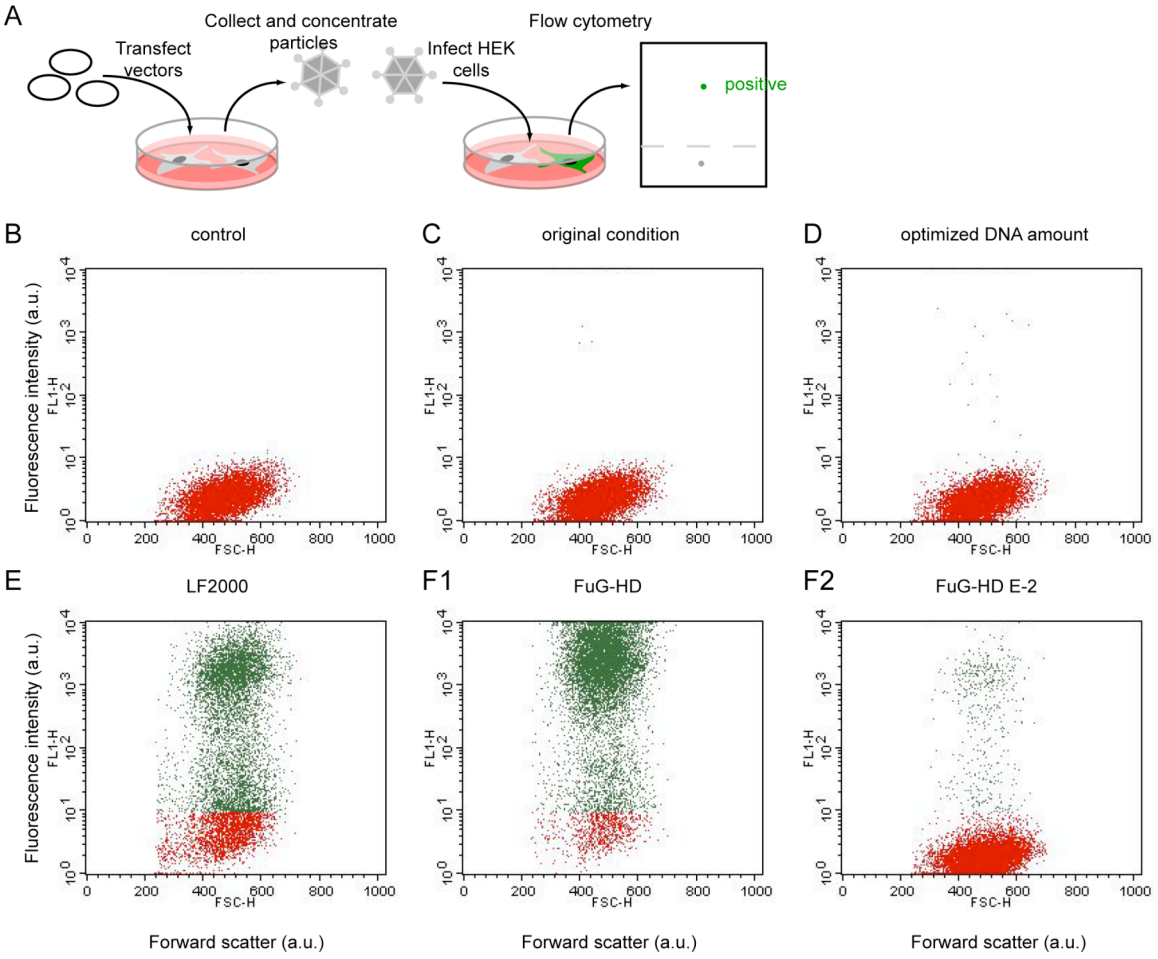

Figure 12 Optimization of lentivirus production in HEK293T cells A) Cartoon depicting lentiviral production and determination of titer. HEK293T cells are transfected with vector carrying the shRNA and GFP as well as the two helper vectors. After incubation viral particles are collected and concentrated. The titer is determined by infecting fresh HEK293T cells. After incubation the fraction of GFP positive cells is determined by flow cytometry. From this fraction the titer is determined. B) Dot blot showing uninfected HEK cells as negative control. Cells with a fluorescence intensity below 10 a.u. are not infected (red). Cells with fluorescence intensity over 10a.u. are positive (green). C) Original conditions reveal few GFP positive cells (green). D) Optimized DNA amounts and ratios increase the particle number. E) Optimized production media and incubation times display striking improvements that are furthermore improved by use of new FuGene HD reagent, limiting the cytotoxcity (F1). F2 depicts 100 fold dilution of F1 to enable accurate titer determination.

Based on an existing protocol (Figure 12C), I first determined the impact of DNA amount and relative ratios. I found that significantly higher amounts of DNA were needed for optimized production (Figure 12D). This came at the expense of elevated cell death in the cultures. To avoid negative effects on the infected

neuronal cultures by factors from less controllable substances - like serum - I established a serum free production medium (Figure 12E). Its additives are similar to those used in neuronal cultures and are based on Neurobasal media. This had no negative effect on particle number. I then minimized cell death resulting from transfection by use of another transfection reagent, FuGene HD. This led to near elimination of cell death due to transfection and significant increase in particle number (Figure 12F1-2). The optimization led to a 1000 fold increase (~$2x10^8$/ml) in particle number over starting conditions (~$2x10^5$/ml).

Infection of hippocampal neuronal cultures with shRNA lentiviruses

I was interested in the effects of acute loss of each of the PSD-MAGUKs on AMPAR targeting to mature synapses. I infected neurons at DIV 15-16 and incubated them for another 5 days post infections and then assayed for knock-down of the protein of interest. As microglia –residual in neuronal cultures – are activated by lentiviruses and cause neuronal cell death, I used mitotic inhibitors to limit their proliferation after infection. Cells can be infected by more than one lentivirus. If too many particles enter a neuron, it will undergo apoptosis. Infection of a cell population is a random process. To achieve infection of the majority of neurons, significantly more virus particles than cells need to be present. These two aspects call for a balance between high infection rate and low levels of cell loss. I found that a multiplicity of infection (MOI) of 2 yields about 70% infection rate with little or no cell death.

Western blot analysis of infected neuronal cultures confirmed that the shRNAs targeting PSD-95, PSD-93 and SAP102 significantly reduce expression of the proteins targeted (Figure 13). NMDAR 1 (NR1) expression was not affected showing specificity of the targeting process. Tubulin bands show that equal amounts of protein are loaded. In contrast, the shRNA targeting SAP97 did not cause significant reduction of its expression (Figure 13 middle right). This was surprising since all four shRNAs selected were comparably effective in the COS-7 cell based assays. I therefore generated a total of eight more shRNAs targeting SAP97 and tested these using four different antibodies specific to SAP97. SAP97 was not knocked down by any of these constructs (data not shown). As shRNA SAP97 was ineffective in neurons, I proceeded with shRNA experiments targeting only PSD-95, PSD93 and SAP102.

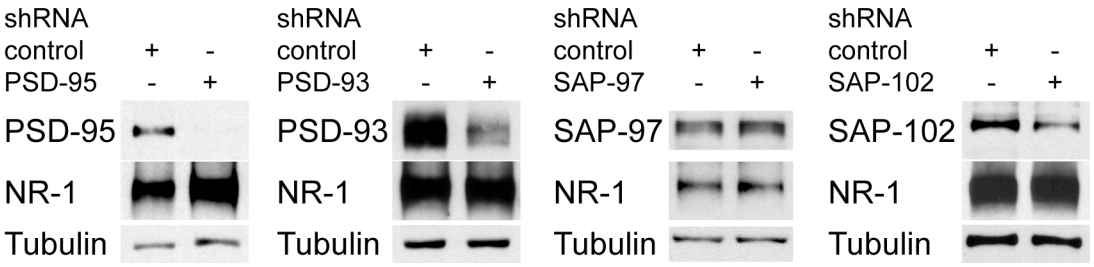

Figure 13 shRNAs knock-down PSD-MAGUKs in hippocampal neuron culture. Dissociated hippocampal pyramidal neuron cultures are infected with lentiviruses (MOI 2) expressing shRNAs. shRNAs targeting PSD-95, PSD-93 and SAP102 knock-down their respective PSD-MAGUKs expression. shRNA targeting SAP97 does not achieve knock-down in neurons. NR-1 expression is not effected. Tubulin is shown as loading control.

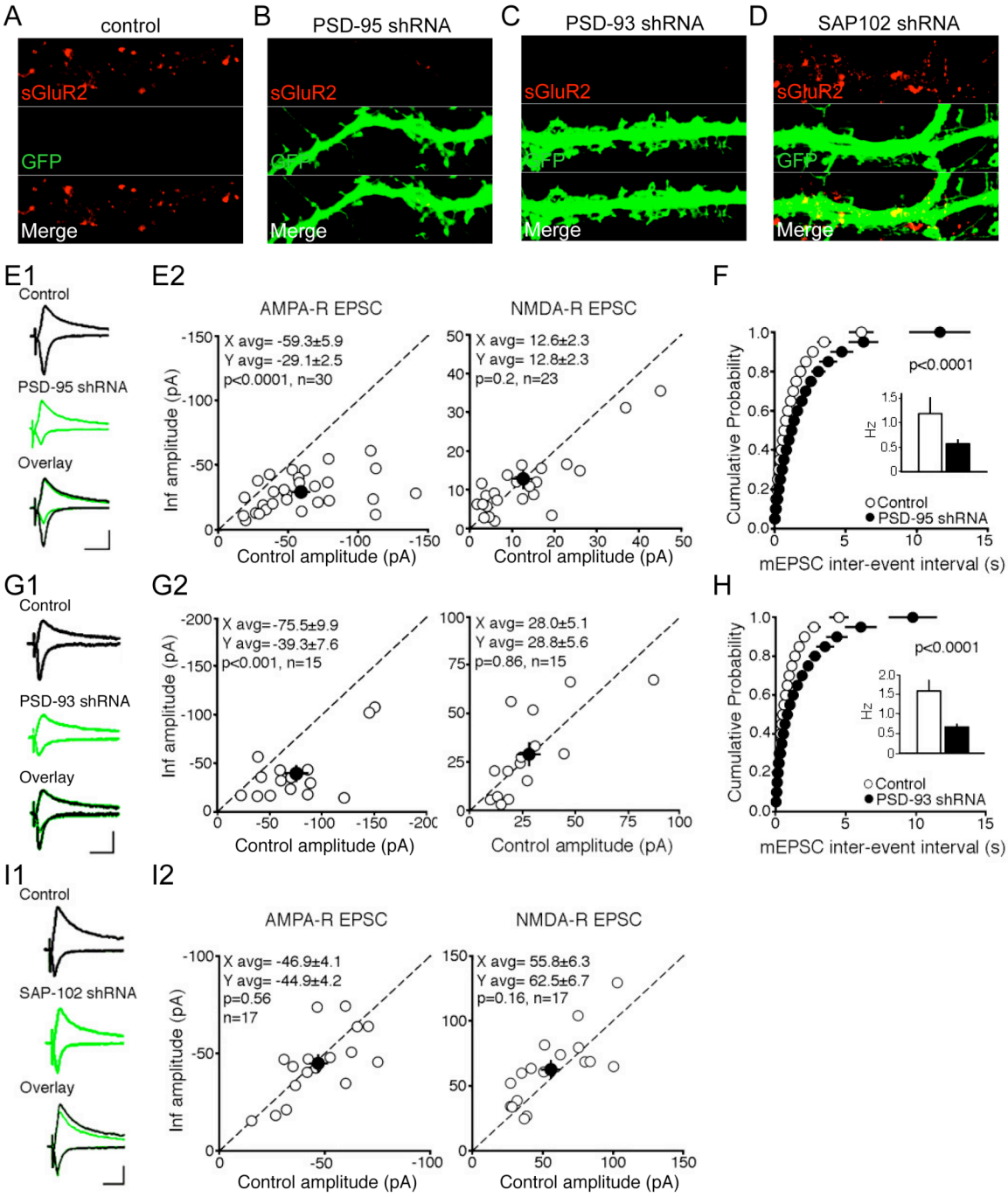

Figure 14 Impaired AMPAR targeting by shRNA PSD-95 and PSD-93. A) A untransfected neighboring cell (DIV21) shows multiple surface GluR2 puncta. B-C) Surface expression of GluR2 is lost from cells transfected with shRNA targeting PSD-95 or PSD-93. D) shRNA SAP102 has no effect on sGluR2 staining in neurons at DIV21. GFP co-expressed by the transfected vector visualizes the morphology. (E1-2, G1-2, I1-2) For scatter plots, open circles represent amplitudes for single pairs and filled circles represent the mean 6 SEM. (E1) Traces of evoked EPSCs recorded simultaneously from an uninfected wild-type neuron (top) and a neighbor infected with PSD-95 shRNA lentivirus (middle). Distributions of EPSC amplitudes show a significant reduction in the AMPAR EPSC (E2) but no change in the NMDA EPSC.F) shRNA-mediated knockdown of PSD-95 does strongly reduce mEPSC frequency with no effect on

mEPSC amplitude (data not shown) ((F), n = 15 pairs). G1) Traces of evoked EPSCs from an uninfected neuron (top) and a neighbor expressing PSD-93 shRNA (middle). Distributions show a reduction in the AMPAR EPSC (G2) but no change in the NMDA EPSC (G2). shRNA-mediated knockdown of PSD-93 does not affect mEPSC amplitude (data not shown), but does reduce frequency ((H), n = 15). I1) Traces of evoked EPSCs from an uninfected wild-type neuron (top) and a neighbor expressing SAP102 shRNA (middle). Distributions of EPSCs show no effect of SAP102 shRNA expression on AMPAR EPSCs (I2) or NMDA EPSCs. Error bars = SEM. (scale bars for E1, G1, I1 50pA; 50ms)

Surface GluR2 staining

Are all PSD-MAGUKs involved in AMPAR expression at the synapse? To test this hypothesis I transfected cultured neurons at DIV 15-16 and incubated for 5-6 more days. Live neurons were incubated shortly with a GluR2 antibody that recognizes the extra cellular N-terminal domain of the receptor. Cells were fixed and stained with fluorescently labeled secondary antibody. This assay visualizes receptors on the surface of the cell only. The short incubation time ensures that only minimal amounts of internalized receptors are detected.

In the control cell, neighboring one of the infected cells, strong sGluR2 puncta are visible along the dendrite (Figure 14A). In shRNA PSD-95 (Figure 14B) and shRNA PSD-93 (Figure 14C) transfected cells sGluR2 puncta are strongly reduced. shRNA against SAP102 does not appear to have an effect on sGluR2 puncta (Figure 14D). This leads to the conclusion that PSD-95 and PSD-93 but not SAP102 are important for surface delivery of AMPARs in matured cultures.

Synaptic transmission of hippocampal neurons

The unique properties of neurons to propagate information in the form of electric currents allows for very sensitive measurements of changes at the

synapse. In collaboration with Roger Nicoll's lab, we assessed the effect of shRNAs against PSD-95, PSD-93 and SAP102 in hippocampal slice culture.

Knock-down of PSD-95 or PSD-93 reduces AMPAR mediated synaptic transmission.

Hippocampal slice cultures were used to examine the effects on synaptic function. Two to three days after preparation, slices were infected with shRNA-carrying Lentivirus and were left for a further 5–8 days. An infected neuron and an uninfected neighbor were simultaneously recorded from and the synaptic responses evoked by a common input compared. A typical experiment is shown by the traces in Figure 14E1. The AMPAR component of the excitatory postsynaptic current (EPSC) was dramatically decreased in the infected cell, whereas there was no difference in the NMDAR component. The results shown in scatter plots for all neuronal pairs demonstrate a 51% decrease in the size of the AMPAR EPSC (Figure 14E2). On the other hand, there is no change in the size of the NMDA EPSC. Using a control shRNA sequence did not effect the AMPAR EPSC (uninfected: 49.1 +/- 6.8 pA; infected: 41.9 +/- 6.5 pA; n = 16, p = 0.29) (data not shown).

To understand the basis for the reduction in AMPAR EPSCs, miniature EPSCs (mEPSCs) were first evaluated. Miniature EPSCs are spontaneous, mono-synaptic events. They arise from a single vesicle fusing spontaneously to the presynaptic terminal. On the postsynaptic side a monosynaptic response can be measured that allows conclusions about the receptor composition of the

single postsynapse. If presynaptic vesicle content is constant, loss of frequency indicates a loss of synapse number. Loss of mEPSC amplitude suggests reduction of synaptic receptor content. In PSD-95 shRNA infected neurons, there was no change in amplitude (data not shown) but a large decrease in event frequency (Figure 14F), suggesting that a population of synapses is silenced. To monitor silent synapses directly, minimal stimulation experiments were carried out to compare the incidence of failures in control and infected cells (data not shown); failure rates were consistently enhanced in the infected cells. In addition, shRNA knockdown of PSD-93 caused a 48% selective reduction in the size of the AMPAR EPSC (Figure 14G1-2), with no change in NMDA EPSCs. To examine the mechanism for this reduction mEPSCs were recorded. Similar to the results with PSD-95 shRNA, depletion of PSD-93 had no effect on the amplitude of mEPSCs (data not shown), but did cause a clear reduction of the frequency of mEPSCs (Figure 14H), suggesting that AMPARs are lost from a subset of synapses, increasing the number of silent synapses.

Previous studies showed, that overexpression of SAP102 selectively enhances AMPAR EPSCs (72). However, knock-down of endogenous SAP102 with shRNA had no effect on basal synaptic transmission (Figure 14I1-2) indicating that SAP102 is not required for synaptic AMPA or NMDAR expression at mature synapses.

PSD-95 and PSD-93 knock-out mice

The results from the use of RNAi contrast with the previously published data, where no effect on AMPAR trafficking in PSD-95 or PSD-93 knock-out mice was found. However, a study conducted on PSD-93 deficient mice focused on cerebella neurons (4). PSD-95 deficient mice show no difference in basal AMPAR transmission but show deficits in plasticity (59). These mice, however, expresses a fragment of PSD-95 including the first two PDZ domains, which obscures the interpretation of the data presented (59, 72). A new and complete PSD-95 knock-out mouse became available (89)(generous gift Prof. S. Grant). Our group had generated the PSD-93 knock-out mouse previously (4). Neither mouse had undergone basic characterization in regard to hippocampal excitatory transmission. I initially examined the expression of related proteins of the postsynaptic density. Western blot analysis showed that both knock-out mice have a complete loss of the targeted protein. Furthermore, expression levels of SAP97, SAP102, GluR1, GluR2/3 and the presynaptic marker synaptophysin are comparable with control littermates (Figure 15A). Tubulin and actin were used as loading controls.

Excitatory synaptic transmission is normal in PSD-93 and PSD-95 knock-out mice

Synaptic transmission was examined in acute hippocampal slices from postnatal day 30 to 40 (P30–40) mice that completely lack PSD-95 protein (89).

Extracellular field potential recordings show comparable strength of synaptic transmission between control and PSD-95 knock-out mice

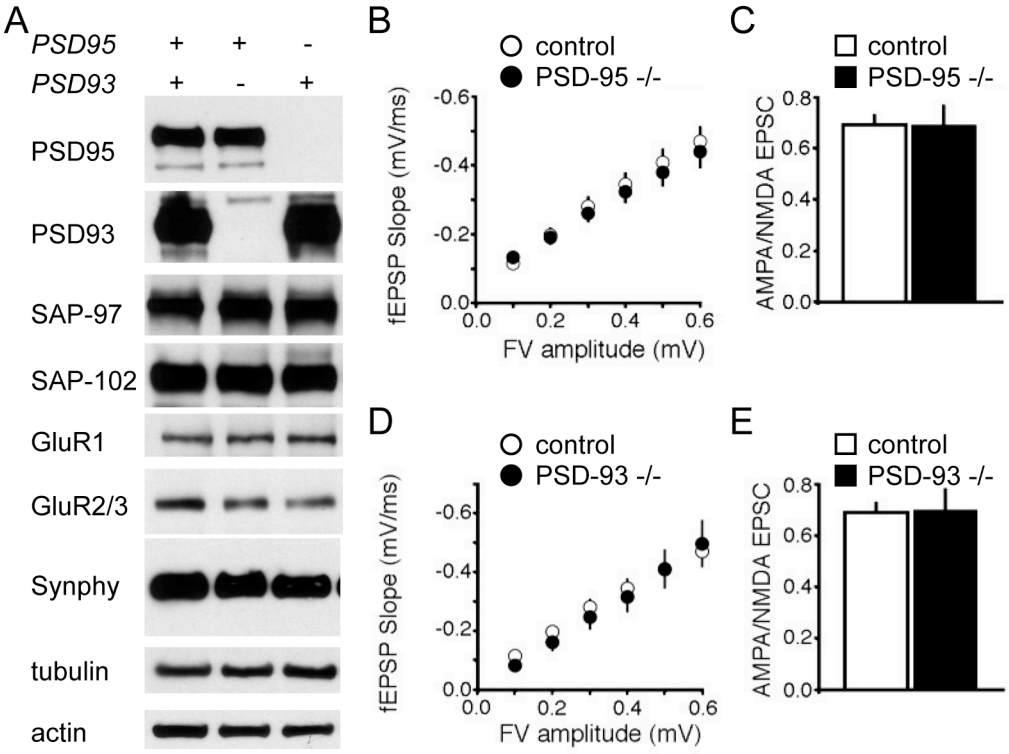

Figure 15 Normal total protein expression and AMPAR mediated transmission PSD-95 and PSD-93 knock-out mice. A) Western blot analysis of hippocampal protein lysates. Lysates from wildtype are compared to PSD-93 and PSD-95 knock-out mice. To confirm genotypes blots for PSD-95 and PSD-93 are shown (top). Expression of related PSD-MAGUKs SAP97 and SAP102 is unaffected by loss of either PSD-95 or PSD-93. Knock-outs express normal amounts of AMPAR subunits GluR1 and GluR2/3 as well as the presynaptic marker Synaptophysin. Tubulin and actin prove equal loading. B) Input-output curve showing that for each input (FV, fiber volley), the output (fEPSP) is unchanged in the PSD-952/2 relative to controls. Each point represents the mean +/- SEM for each fiber volley (controls, n = 56; PSD-95 knock-out, n = 26; p > 0.05 for all fiber volleys). C) Bar graphs showing no difference in the AMPA/NMDA EPSC ratio (controls: 0.69 +/- 0.04, n = 40; PSD-95 knock-out: 0.69 +/- 0.08, n = 20; p = 0.94). D) Input-output curve showing that for each fiber volley the fEPSP is unchanged in PSD-93 knock-out (controls: n = 56; PSD-93 knock-out n = 16). p > 0.05 for every fiber volley. E) Bar graphs showing no difference in the AMPA/NMDA EPSC ratio (control: 0.69 6 0.04, n = 40; PSD-93 knock-out: 0.7 6 0.08, n = 11; p = 0.92). Error bars = SEM.

. The size of the presynaptic fiber volley (input) was compared to the size of the field excitatory postsynaptic potential (fEPSP) response (output). Over a range of stimulus strengths, no differences were observed between PSD-95

knock-out and control mice (Figure 15B). Next, the size of the AMPAR EPSC to that of the NMDA EPSC was compared. In contrast to the shRNA experiments, no difference in the AMPA/NMDA EPSC ratio was found (Figure 15C), indicating that synaptic transmission is normal in the PSD-95 knock-out mouse.

Furthermore, synaptic transmission in the hippocampus of the PSD-93 knock-out mouse (4) was analyzed. Use of field potential recordings evaluated the strength of synaptic transmission. No difference in synaptic strength was found (Figure 15D). Next, the relative contribution of AMPA and NMDARs to the synaptic response was examined (Figure 15E); again, no difference could be detected. These results directly contradict the results obtained by using shRNA against PSD-95 and PSD-93. Might loss of one of these proteins be compensated for by the others?

Specific binding partners of PSD-95 and PSD-93

The results suggest that PSD-95 and PSD-93 have overlapping as well as distinct functions. Alignment analysis reveals unique sequences for each protein. I wanted to examine if specific binding partners for each protein exist. I first examined available antibodies for their usefulness in immunoprecipitation experiments. I used a pan-PSD95/93, a PSD-95 and a PSD-93 specific antibody and compared these to control IgG. The pan as well as the PSD-93 specific antibody proved useful for this experiment (Figure 16A-B).

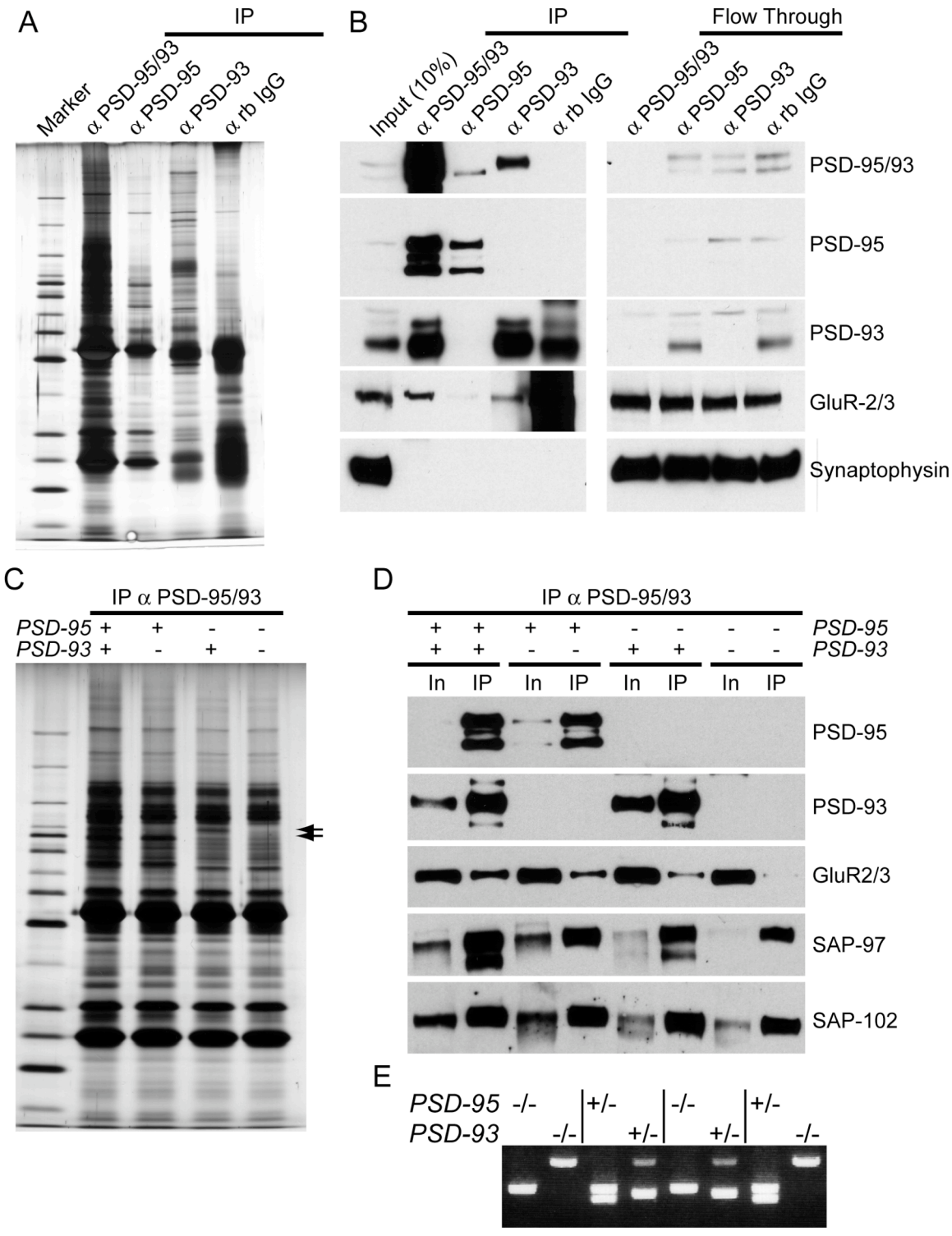

Figure 16 Preparative Immunoprecipitation of PSD-95 and PSD-93 from hippocampus. A) Silver stained preparative protein gel shows a multitude of specific bands precipitated with equal amounts of pan-PSD-95/93, PSD-95 and PSD-93 antibodies. Unspecific IgG is used in control conditions. B) Western blots confirm precipitation of key proteins. The pan-PSD95/93 antibody shows strong precipitation of PSD-95 and PSD-93 as well as co-precipitation of GluR2/3, a known binding partner. PSD-95 specific antibody precipitates with only low efficiency. The

corresponding flow-through lane (right panel) still contains significant amounts of PSD-95. Thus this antibody is excluded from further experiments. PSD-93 specific antibody precipitates specifically and efficiently. GluR2/3 is co-precipitated. Flow through lane does not show any PSD-93. The presynaptic marker synaptophysin does not precipitate with either antibody. C) Silver stain of pan-PSD95/93 precipitated lysates from control littermates, PSD-95 KO, PSD-93 KO or PSD-95/PSD-93 double KO. Two distinct bands, representing PSD-95 and PSD-93 (arrows), are lost in lysates from PSD-95, PSD-93 or double knock-out mice. Other distinct bands can be identified. D) Western blot analysis shows the efficient precipitation of PSD-95 and PSD-93 and confirms genotypes. GluR2/3 co-precipitate from control and single knock-out lysates. Unanticipated precipitation of SAP97 and SAP102 in all lysates – including the double knock-out – complicates the analysis and might explain the extremely high background in the silver stain. Thus it is concluded that the pan-PSD-95/93 antibody also detects SAP97 and SAP102 in this experiment also not obvious in western blot of lysates. E) Representative agarose gel of PSD-95 and PSD-93 genotype PCR. Genotypes for PSD-95 and PSD-93 are determined in one PCR reaction with two products each. Larger product identifies presents of KO allele, bottom for the wild type allele, for both genes. Individual animal samples are separated by vertical lines. (-/- knock-out, +/- heterozygous)

The AMPAR subunits GluR2/3 were precipitated with these antibodies. Making use of the single as well as the double knock-out mice I performed immunoprecipitations with the pan-PSD-95/93 antibody. In this experimental design all conditions are constant with the exception that PSD-95 and/or PSD-93 are absent from the lysates of respective knock-out animals. Their respective binding partners will therefore be absent from precipitates, allowing identification of common and specific binding partners as well as unspecific binding in the lysates of double knock-out animals. Silver staining reveals loss of two bands identified as PSD-95 and PSD-93 in the respective knock-outs (Figure 16C). Apart from this no specific bands could be identified. Western blot analysis reveals that PSD-95 and PSD-93 were precipitated very efficiently. GluR2/3 was also detected in the precipitates. Unfortunately the pan-PSD95/93 also precipitated SAP97 and SAP102 (Figure 16D). Thus the analysis is convoluted by precipitates bound to these two proteins. Interestingly, the precipitated amount of GluR2/3 appears to decline significantly with the subsequent loss of either PSD-95 or

PSD-93 and both, suggesting AMPARs might mostly be bound to these two PSD-MAGUKs (Figure 16D).

The Effects of Gene-Targeted Double Knockout (DKO) of PSD-95 and PSD-93 on Synaptic Transmission

As shRNA to either PSD-95 or PSD-93 diminish synaptic targeting of AMPARs, perhaps functional redundancy masks synaptic deficits in the single KO mice. To address this, I generated PSD-95/PSD-93 double KOs. Unlike the single KOs, which were grossly indistinguishable from their littermates, PSD-95/PSD-93 double knock-out mice were clearly impaired. By 3 to 5 weeks of age, these animals were noticeably smaller than control littermates (Figure 17F) and typically died unless special care was provided from weaning onward. The animals had impaired gait and were markedly hypokinetic.

Western blot analysis of PSD-95/PSD-93 double knock-out hippocampal homogenates and littermate controls showed no difference in the total amounts of GluR1, GluR2, and NR-1 (Figure 17A1-2). However, the PSD-enriched fraction (TritonX100 insoluble) showed ~45% loss of GluR1 and GluR2 (Figure 17B1-2), while NR-1 remained unchanged.

In accord with the biochemical data field input/output curves in these animals revealed a 55% reduction in synaptic transmission (Figure 17C). Furthermore, the AMPA/NMDA EPSC ratio was reduced ~50% (Figure 17D). These decreases occurred without any change in paired pulse facilitation (PPF) (data not shown), indicating that the probability of transmitter release was

unaltered. Interestingly, as with shRNA knockdown of PSD-95 or PSD-93, the amplitude of mEPSCs was unchanged (data not shown), but there was a dramatic reduction in the frequency (Figure 17E).

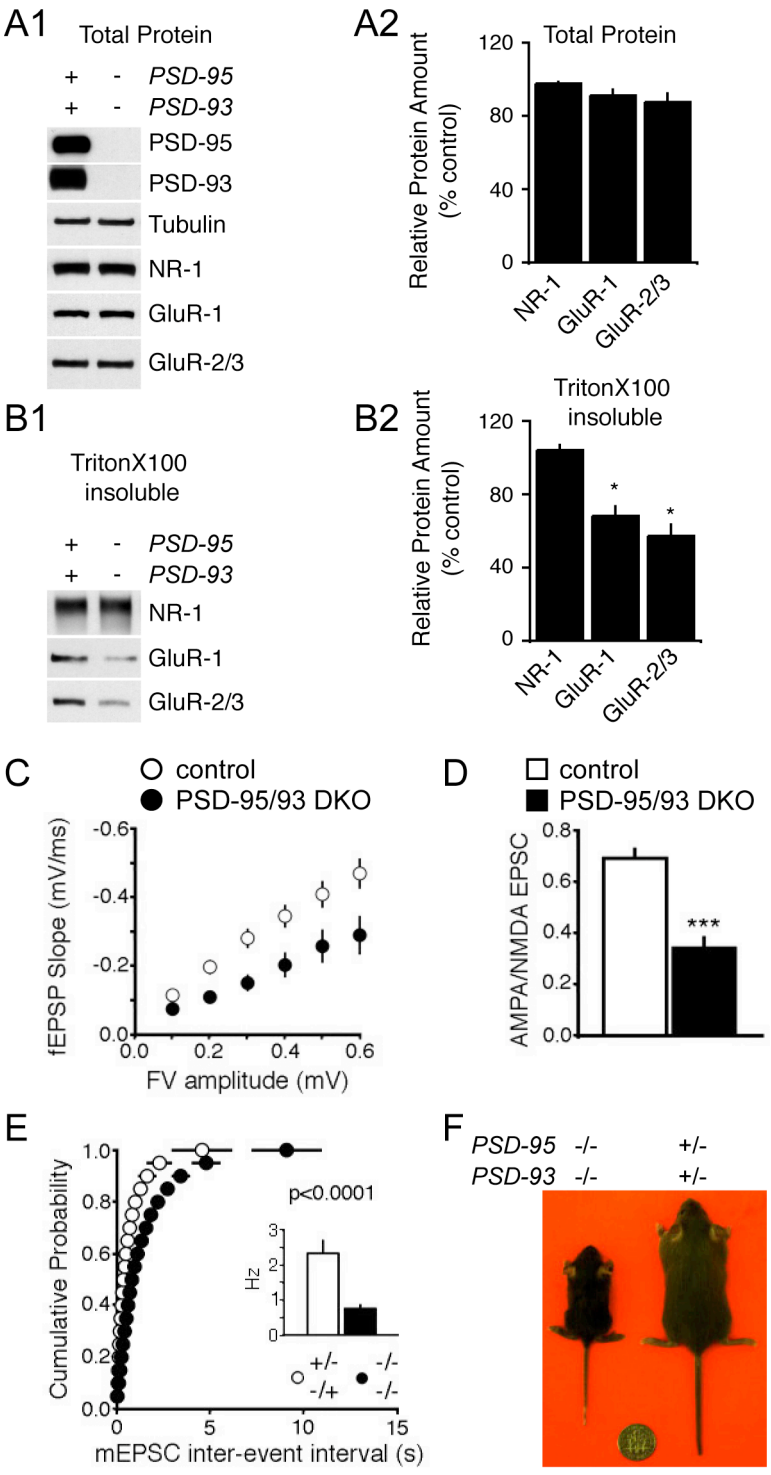

Figure 17 Impaired synaptic AMPAR targeting in PSD-95/PSD-93 double knock-out A) Normal total protein expression of glutamate receptors in hippocampus of PSD-95/PSD-93 double knock-out mice. A1) Western blots confirm absence of PSD-95 and PSD-93 in hippocampal total protein lysates. Expression levels for GluR1, GluR2/3 and NR1 are comparable in double knock-out and control animals. Tubulin blot shows equal protein amount. A2) Quantification of glutamate receptors GluR1, GluR2/3 and NR1 in total protein hippocampal lysates. B1) Western blots of PSD enriched, TritonX100 insoluble, fraction show loss of GluR but not NR receptor subunits. B2) Quantification of western blots for glutamate receptor subunits. GluR1 and GluR2/3 but not NR1 are significantly reduced in PSD enriched fractions (error bars = SEM). C) Input-output curve showing a reduction in the input-output relation in PSD-95/PSD-93 double knock-out (DKO) (controls: n = 56; PSD-95/PSD-93 DKO: n = 15; $p < 0.05$ for FV = 0.2–0.6). D) AMPA/NMDA EPSC ratio bar graphs showing a reduction in PSD-95/PSD-93 double knock-out mice (control: 0.69 6 0.04, n = 40; PSD-952/2/PSD-932/2: 0.34 6 0.04, n = 8; ***$p < 0.001$). E) mEPSC cumulative probability distributions showing a significant reduction in mEPSC frequency in PSD-95/PSD-93 double knock-out mice (control: n = 16; PSD-952/2/PSD-932/2: n = 13). F) P32 PSD95 -/-/PSD-93 knock-out double knock out and littermate control.

Where do AMPARs locate if they are not anchored at the synapse? To address this question I examined the solubility of AMPARs in the double knock-out compared to heterozygous littermate controls. Hippocampal membrane fractions were solubilized in 1% TritonX100 buffer. The insoluble fraction is separated by ultracentrifugation. This fraction is then solubilized using 1% SDS buffer. In this SDS soluble fraction, synaptic proteins are enriched. Western blots of this experiment show that AMPARs are redistributed away from the synaptic enriched fraction to extra synaptic membranes (Figure 18). Interestingly, SAP102 appears to be redistributed to the synaptic fraction indicating a compensatory mechanism.

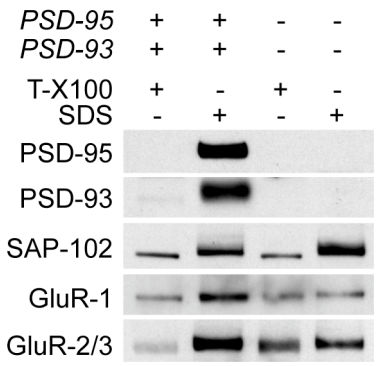

Figure 18 Redistribution of AMPAR subunits from the synaptic fraction. Membrane fractions from PSD-95/PSD-93 double knock-out and control hippocampal homogenates are solubilized in 1% TritonX100. The insoluble fraction is treated with 1% SDS. This fraction is PSD enriched. PSD-95 and PSD-93 are almost exclusively found in the PSD enriched fraction. GluR-1 and GluR-2/3 redistribute from the PSD enriched to the TritonX100 soluble membrane fraction in PSD-95/PSD-93 double knock out mice.

Role of SAP102 in Synaptic Transmission

What might account for the remaining transmission in the PSD-95/PSD-93 double knock-out mice? As this remaining transmission greatly exceeds the subtractive effects of the combined individual shRNA-mediated knock-downs, some type of compensation has presumably occurred. Might other PSD-MAGUKs contribute to clustering synaptic AMPARs? I first carried out western blot analysis on hippocampal homogenates from PSD-95/PSD-93 double knock-out mice and found no change in the total level of SAP97, whereas SAP102 expression was increased by about 20% (Figure 19A1-2). Similar results were obtained for the PSD-enriched fraction (Figure 19B-2). These results suggest that SAP102 may cluster the AMPARs mediating the remaining synaptic transmission.

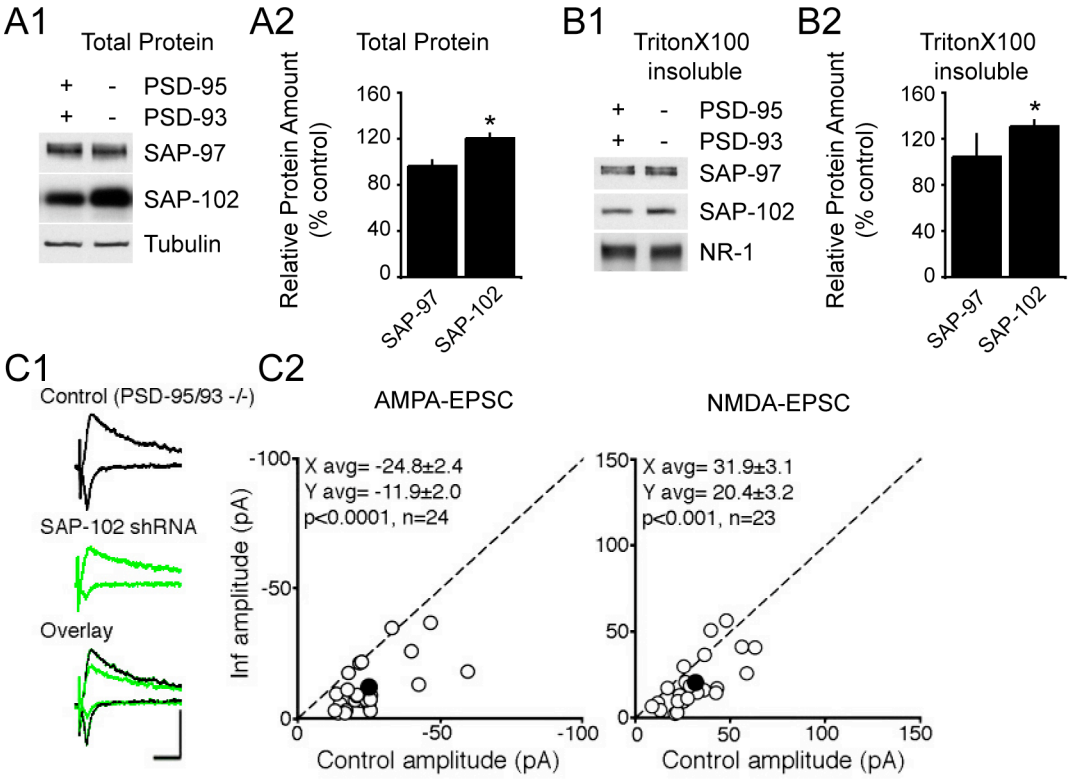

Figure 19 SAP102 compensates for loss of PSD-95 and PSD-93. A1) Western blots from total hippocampal protein lysates show upregulation of SAP102 but not SAP97 in PSD-95/PSD-93 double knock-out mice. A2) Densitometry quantification of western blots of total hippocampal lysates. SAP102 is significantly upregulated in double knock-out compared to litter mate controls. B1) Western blots of PSD enriched, Triton-X100 insoluble, fraction show specific SAP102 upregulation. SAP97 and NR1 are unaltered. C1) Traces of evoked EPSCs from an uninfected PSD-95/PSD-93 double knock-out neuron (top) and a neighbor expressing SAP102 shRNA (middle). Distributions of EPSCs show that SAP102 knockdown reduces the AMPAR EPSC and modestly reduces the NMDA EPSC. Scale bars for (C1) and (D1), 25 pA, 50 ms. C2) Open and filled circles represent amplitudes for single pairs and mean +/- SEM, respectively.

Previous studies showed that overexpression of SAP102 selectively enhanced AMPAR EPSCs (72). However, knockdown of endogenous SAP102 with shRNA had no effect on basal synaptic transmission (Figure 14I1-2), indicating that SAP102 is not required for synaptic AMPAR or NMDAR expression at mature synapses. In striking contrast SAP102 shRNA expression in slice cultures from PSD-95/PSD-93 double knock-out mice caused a 52% reduction in the remaining transmission (equivalent to 82.5% from wild-type) (Figure 19C1-2).

There was also a small reduction in the NMDAR component (Figure 19C2). No change in PPF was detected, indicating a postsynaptic change. Concomitant with the reduction in evoked synaptic transmission, AMPAR-mediated mEPSC amplitude was decreased and frequency was further decreased, suggesting removal of AMPARs from all of the remaining synapses.

I assessed the developmental profile of these three PSD-MAGUKs from postnatal day P5 to P32 in western blots. PSD-95 and PSD-93 start to be expressed around P11 to P15 (Figure 20A). Their expression plateaus at about P26. In contrast SAP102 is strongly expressed at P5 and decreases over time. There appears to be a switch of PSD-MAGUKs around P15. The onset of impairment in PSD-95/PSD-93 double knock-out mice matched this developmental expression profile. Thus, one week old PSD-95/PSD-93 double knock-out mice were indistinguishable from their littermates.

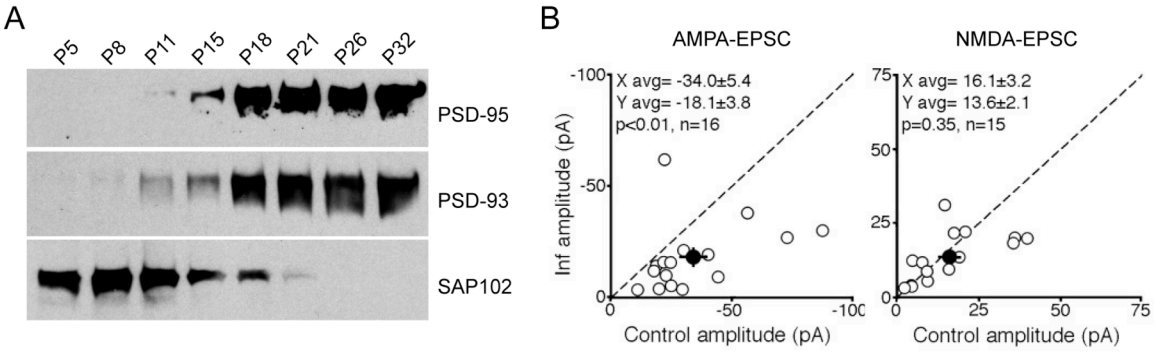

Figure 20 SAP102 controls AMPAR trafficking in early postnatal development. A) Western blots of total hippocampal lysates from wild type mice show development of PSD-MAGUK expression. PSD-95 and PSD-93 appear first at P11 and peak at P21 and are continuously expressed thereafter. SAP102 is expressed early on and declines later. This pattern suggests a developmental switch of PSD-MAGUKs during postnatal development. B) Distributions of EPSC amplitudes show a significant reduction in the AMPAR EPSC in cells expressing SAP102 shRNA with no change in the NMDA EPSC.

Moreover, 1 week old PSD-95/PSD-93 double knock-out mice showed no difference in the AMPA/NMDA ratio, mEPSC amplitude, or mEPSC frequency. Whereas SAP102 shRNA had no effect on mature synapses (Figure 14I1-2), SAP102 shRNA caused a ~50% reduction specifically in AMPAR-mediated synaptic transmission in immature synapses (Figure 20B). This establishes SAP102 as the dominant PSD-MAGUK for AMPAR trafficking during early postnatal development.